Homopolymers as Structure-Driving Agents in Semicrystalline Block Copolymer Micelles

Georgios Rizis, Theo G. M. van de Ven,* and Adi Eisenberg*

Department of Chemistry, McGill University, 801 Sherbrooke Street West, Montreal, Quebec, Canada H3A 0B8 and Centre for Self-Assembled Chemical Structures (CSACS), Montreal, Quebec, Canada H3A 2K6

ABSTRACT A simplified hierarchical self-assembly strategy is presented in which homopolymer additives are used to manipulate the crystallization-driven self-assembly of block copolymer micelles in selective media. By first incorporating the appropriate homopolymer chains within the micelle core, the system then evolves passively to yield crystalline platelets. These lamellae may be considered as self-assembled analogues of the traditional polymeric single crystal, which can be challenging or laborious to obtain otherwise. Used here as the test systems are micelles bearing polycaprolactone as the crystalline subphase in water and a mixed hydrophilic corona of poly(ethylene oxide) and poly(acrylic acid) the composition of which was varied methodically. Comicellization with homo-PCL has no influence at first; instead, the assemblies undergo morphological changes hierarchically, which were probed by electron microscopy and light scattering measurements. For all materials, the final product is consistently lamellar and micrometer-sized; however, lamellar shape variations are encountered as the stabilizing corona is altered. Such lamellae are unexpected based on the composition of most copolymers used here. The phenomenon also depends highly on the nature of the homo-PCL additive. A possible source for the activity of the homo-PCL is suggested, which also provides a strong basis to adapt the strategy for other crystalline materials.

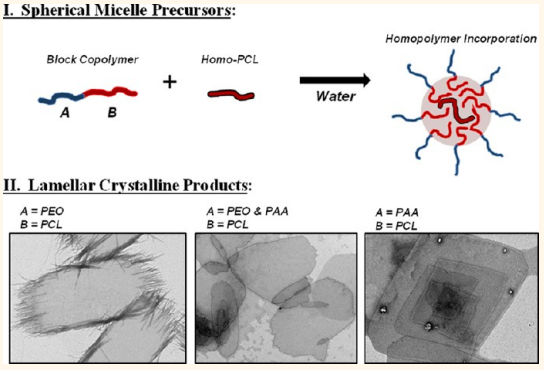

KEYWORDS: block copolymers · core-crystalline micelles · lamellae · hierarchical self-assembly

Block copolymers are macromolecules that consist of two or more chemically distinct polymeric segments joined together covalently. Their self-assembled nanostructures have widespread applications in areas ranging from energy, to catalysis, to medicine.[1−3] In the solid state, nanoscale order can arise when dissimilar polymer blocks segregate into different domains. In solution, self-assembly is driven by the minimization of unfavorable interactions between the solvent and the insoluble polymer blocks. Recent work using hybrid,[4−8] multicomponent,[9−14] or stimuli-responsive materials[15−19] has expanded the toolbox of structures accessible in solution considerably. Now targeting structures that are increasingly complex, researchers strive toward new methods in self-assembly that must be ever more simplified, yet highly robust.

In some systems, crystallization-driven self-assembly has been used to create an impressive range of hierarchical block copolymer nanostructures.[20−27] Although the underlying physical principle, crystallinity, is not unique to any single block copolymer type, there are still relatively few examples where structural features, such as the aggregate morphology, can be controlled readily. The traditional example of a polymeric crystal is the chain-folded single-crystalline lamella; these structures are obtained typically through recrystallization or seeded growth protocols, which have been successful for many polymers, but can be stringent and difficult to develop due to special solvent and temperature considerations.[28,29] Like crystals of most materials, the operative growth mechanism involves the addition of individual molecules to growing crystals or nuclei. The crystallinity of block copolymers is more complex, as crystallization and micellization can take place concurrently, yielding micelles with crystalline or semicrystalline

* Address correspondence to theo.vandeven@mcgill.ca, adi.eisenberg@mcgill.ca.

Received for review September 8, 2014 and accepted March 11, 2015.

Published online March 11, 2015
10.1021/nn505068u

cores. Composition-dependent trends have been examined for several materials.[24,30−32] Mechanistically, some block copolymer systems have shown evidence of a nonclassical crystal growth pathway whereby the micellar objects themselves associate to form a single-crystalline suprastructure.[33−37] This particle-based crystallization mode, while controversial in block copolymer science, is analogous to phenomena that are now recognized within biomineralization,[38,39] protein crystallization,[40] and among inorganic nanocrystals.[41] Hallmarks of particle-based growth are found occasionally in the crystalline micellar products, which can result in unique shapes; representative examples include fringed platelets bearing rod micelle-like protrusions at the edges,[34] and hyper-branched 2D fractal aggregates of spheres.[36,37] Given the vast synthetically accessible range of materials already available at present,[42−45] block copolymers are especially versatile model systems for the study of nanocrystalline behavior.

The environment within a self-assembled structure can be severely confined, which would impose a number of constraints on crystallization.[46−48] Compared to block copolymer chains, which experience restrictions due to their attachment to an incompatible polymer block, homopolymers should be able to crystallize more effectively within nanoscale volumes. Experimentally, the latter concept has been tested, for instance, through the clever use of photocleavable block junctions in solid state samples.[49,50] In solution, the introduction of homopolymers can create an analogous situation within the core of a micelle. While effects on the crystalline properties of the core can be expected, these would be especially difficult to characterize when working with a colloidal system. More challenging still would be to anticipate how any possible differences in these crystalline properties might influence the morphology.

Homopolymers have been used before in crystalline systems, and can indeed be highly effective in manipulating the properties of block copolymer assemblies.[51−53] Recently, we demonstrated a new self-assembly method which makes use of crystallizable homopolymer chains to gain access to a series of hierarchical block copolymer structures.[54] In the latter preliminary work, we investigated spherical micelles of poly(ethylene oxide)-*block*-polycaprolactone (PEO-*b*-PCL) in water, which were loaded with homo-PCL chains during micelle formation. Through a sequence of ordered aggregation events, these spheres transform into rods and, ultimately, micron-sized lamellae that were shown to be close structural analogues of chain-folded PEO-*b*-PCL single crystals.[55,56] The nature of the final product depends entirely on the amount of homopolymer added to the system initially; spheres, rods, ribbons and lamellae can all be prepared from a given PEO-*b*-PCL copolymer, and the lamellar aspect ratio is controllable. The desired product evolves directly in water, predictably, with no need to vary the environmental conditions to begin, or to regulate, the growth process. In this approach, the homo-PCL seems to accentuate crystallinity-driven transformations, as if somehow catalyzing a set of energy-lowering morphological ripening processes that would not occur normally on an observable time scale.[57] Beyond just the range of structures made available this way, in examining this particular micellar system, we uncovered a novel mechanism of lamella formation. Formed by aligning elongated rods both in length and in a plane, these block copolymer lamellae are produced through a two-dimensional (2D) self-assembly pathway seen for no other material before.

In the present article, we test the generality of the method summarized above by comparing the morphological effects of homo-PCL on a series of different aqueous micellar systems. Using mixtures of two different copolymer types, we first made systematic changes to the composition of the hydrophilic corona by substituting the non-ionic PEO for polyelectrolyte blocks of poly(acrylic acid) (PAA). We report on a range of product structures, all obtained by using homo-PCL, and document morphological features as a function of the corona composition and of the solution pH, while exploring preparative variations that affect the hierarchical self-assembly process. We then focus more specifically on the action of the homo-PCL component. Using PEO-*b*-PCL spheres as the test system, we describe the effects of different homo-PCL additives on the morphology, and discuss mechanistic aspects that might permit the expansion of our strategy to a range of other polymer types.

RESULTS

For the present study, the initial micellar structures were prepared by adding water to a polymeric solution in an organic solvent. Through dialysis, these micelles could then be isolated in pure water. In a first set of experiments, we compared the postmicellization behavior of hybrid structures formed from binary block copolymer mixtures (components: PEO_{45}-*b*-PCL_{24} and PAA_{57}-*b*-PCL_{47}; subscripts give the number average of repeat units), in the presence/absence of a third polymeric component (PCL_{10} homopolymer), which could be incorporated within the micelle core upon assembly. More detailed molecular characteristics of these materials, and of all other block copolymer and homopolymers are provided in Tables SI-1 and SI-2 of the Supporting Information, respectively. The desired blending ratio was established by mixing solutions of each desired component before forming the hybrid micelles. The starting morphology of these *bis*-hydrophilic hybrids was spherical for all blends investigated here; these structures consist of a PCL core surrounded by a hydrophilic shell composed of PEO and PAA in regulated proportions (see Table SI-3 in the Supporting

Information for further details). We begin by describing the behavior of the hybrid micelles and the effects of the PCL_{10} additive on the morphology. We present next the results obtained when mixing together two separate preformed micelle populations, each one made using a single block copolymer, either alone or coassembled with PCL_{10} chains. A graphical summary of these experimental procedures is provided in Scheme 1.

Spherical aggregates were obtained by coprecipitating mixtures of up to three polymeric components, dissolved together in dioxane, through the addition of water (chemical structures are shown at center; color coding is blue for PEO, red for PCL, and green for PAA). Hybrid micelles (shown on top) present a *bis*-hydrophilic corona of PEO and PAA chains, the ratio between which is adjustable. Hybrid micelle controls (left) exhibit negligible changes, whereas hybrids containing homo-PCL (right) evolve to yield lamellae (see Figures 2 and 3). Single-copolymer samples (shown below) were also prepared with or without homo-PCL; the individual micelle populations were then mixed together and allowed to coevolve into *bis*-hydrophilic lamellae (see Figure 4). Possible variations, such as changes to the polymer block lengths, the homo-PCL length and content, the proportion of each micelle population, and the use of hybrids in micelle mixture experiments, offer far more options for self-assembly than were probed in this work.

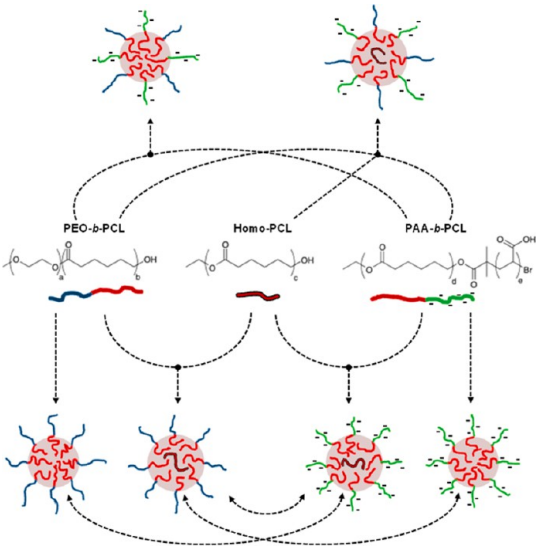

Scheme 1. Summary of *bis*-Hydrophilic Sample Preparation from Free Chains to Primary Spheres

Previously, we documented a set of gradual morphological changes affecting PEO-*b*-PCL spheres during storage in pure water.[57] These changes are linked to the crystallization of the PCL micelle core, which destabilizes the spheres in favor of elongated rods or ribbon-like products. The transformation rates were found to be remarkably consistent when using the same material, but vary when the block lengths are changed. For the hybrid micelles investigated here, we found qualitatively similar behavior; TEM images of rod-like products observed in aged hybrid micelle samples are shown in Figure SI-1 of the Supporting Information. Regarding the kinetics, we found that spheres made of PAA_{57}-*b*-PCL_{47} alone do not transform and are, thus, stable in water; however, when coassembled with PEO_{45}-*b*-PCL_{24}, the hybrid micelles exhibit incrementally slower transformation rates as the fraction of PAA_{57}-*b*-PCL_{47} is increased. Stability trends for the hybrid micelles can be obtained from light scattering intensity and DLS measurements performed as a function of time; a representative example is presented in Figure 1.

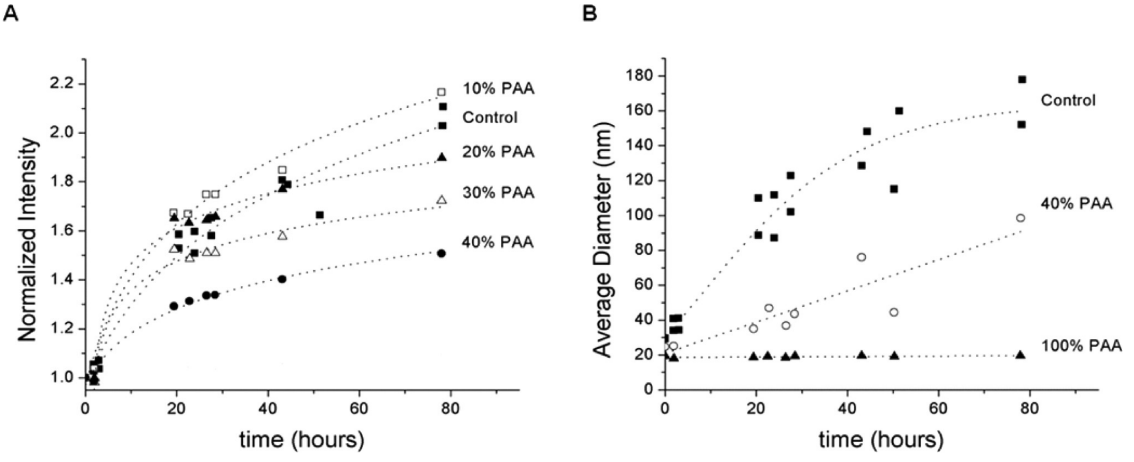

Figure 1. Hybrid micelles prepared without homopolymer additives. (A) Evolution of light scattering intensity with time for hybrid sphere samples made of PEO_{45}-*b*-PCL_{24} and PAA_{57}-*b*-PCL_{47} block copolymers. The fraction of PAA_{57}-*b*-PCL_{47} chains is indicated next to each curve. Note that changes are greatest at low PAA content. (B) Evolution of the average apparent particle diameter with time for selected samples from (A), and for the PAA_{57}-*b*-PCL_{47} control. The diameters were estimated from DLS data; the fitting was performed by the method of cumulants; measurements were performed at a scattering angle of 90°.

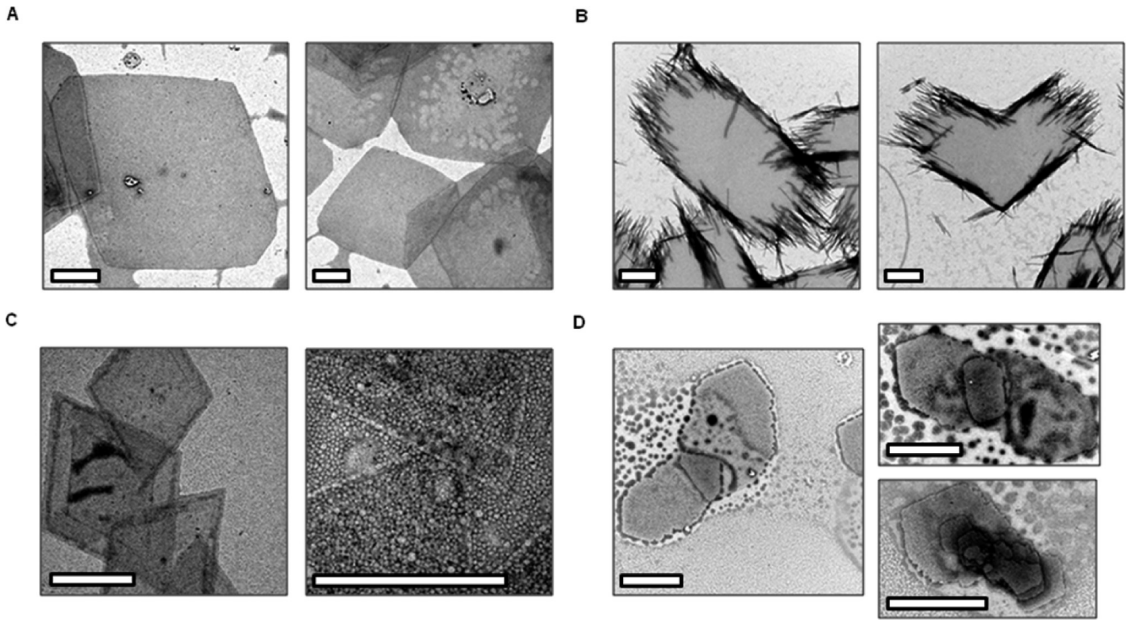

Figure 2. Representative TEM images of lamellae obtained from single-copolymer samples in the presence of PCL_{10} homopolymer. (A) Sharp-edged platelets obtained with PAA_{57}-*b*-PCL_{47}. (B) Fringed "raft"-type lamellae obtained with PEO_{45}-*b*-PCL_{24}. Lamellar products obtained in pH modulation experiments from samples pretreated with (C) CsOH and (D) HCl. Note the altered appearance under acidic conditions. With the exception of (C), all images were enhanced through negative staining with phosphotungstic acid (see text for details). Scale bar: 1 μm.

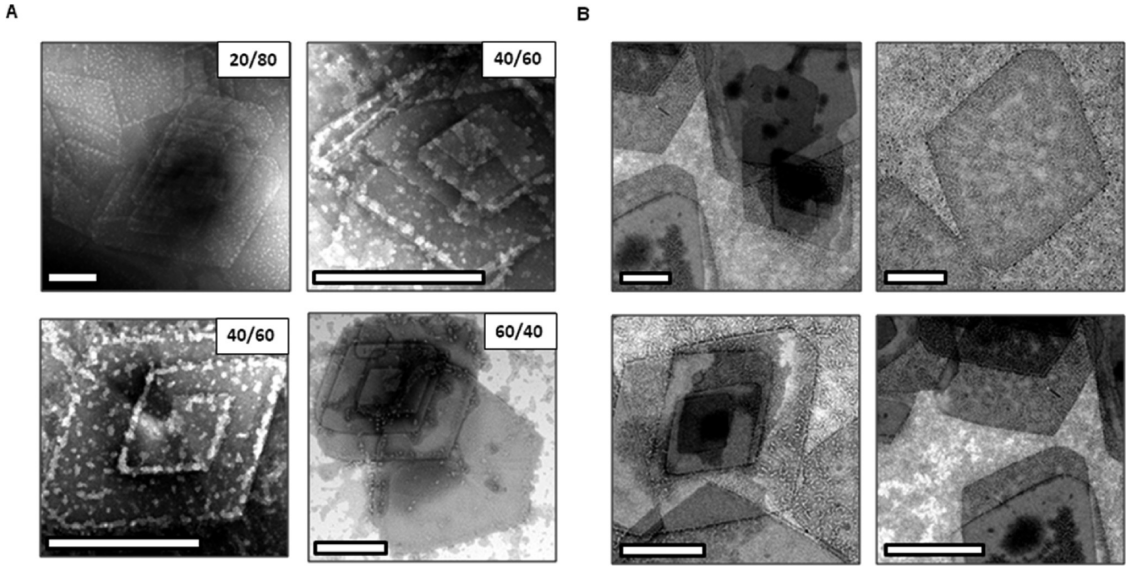

Figure 3. Representative TEM images of lamellae obtained from *bis*-hydrophilic samples in the presence of PCL_{10} homopolymer. Similar lamellar products were found in (A) hybrid micelle samples of PAA_{57}-*b*-PCL_{47} and PEO_{45}-*b*-PCL_{24} (relative proportion indicated in top right corner), and (B) micelles prepared using the triblock copolymer PEO_{45}-*b*-PCL_{37}-*b*-PAA_{72}. Scale bar: 1 μm.

Taken alone, these kinetic trends would suggest a major influence due to the electrostatic repulsion arising from charged PAA chains on the micelle surface: the more PAA-rich samples are also the most stable. However, further experiments show that the stabilizing effect must not be due to this repulsive force alone. For example, single-component spheres of PAA_{57}-*b*-PCL_{47}, which are stable in pure water, also show no transformations when kept in acidic media; the pH value, specifically, was kept two units lower than the nominal pK_a of the acrylic acid groups in an attempt to eliminate most of the charges (see Figure SI-2 in the Supporting Information). Similarly, no effect on the stability was observed when these spheres were kept in 0.1 M aqueous KCl, which should screen and attenuate the surface charge effects. In the case of the hybrid micelles, we tune the electrostatics by substituting of some amount of charged PAA_{57}-*b*-PCL_{47}

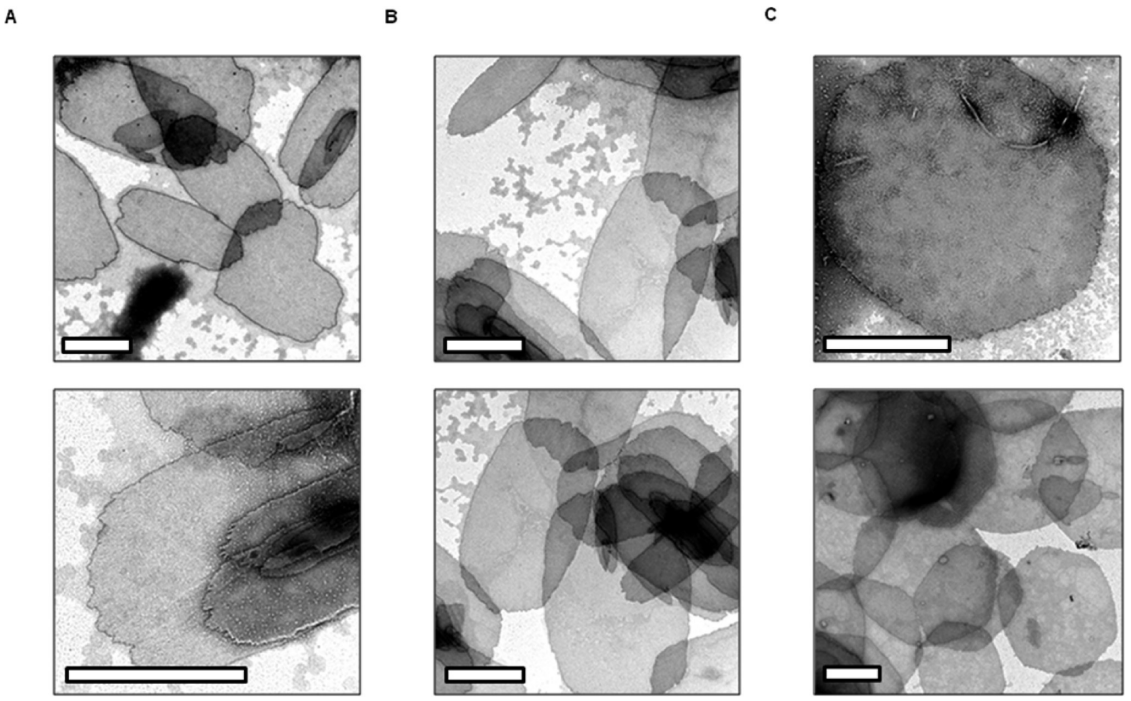

Figure 4. Representative TEM images of lamellae obtained from mixed preformed spherical micelle populations. Each sample combines two individual sphere populations, one prepared from only PAA_{57}-*b*-PCL_{47} and the other from only PEO_{45}-*b*-PCL_{24} block copolymers, mixed together at equal weight concentrations. The homopolymer-loaded populations contain 10% (w/w) PCL_{10}. For (A) and (B), the PCL_{10} is carried by only PAA_{57}-*b*-PCL_{47} and PEO_{45}-*b*-PCL_{24} spheres, respectively. Note the similar appearance of the final products. For (C), both sphere populations harbor PCL_{10} chains. Scale bar: 2 μm.

chains for non-ionic PEO_{45}-*b*-PCL_{24} chains; the lowered pH, therefore, should have a much stronger effect on the micelle surface charge, yet the hybrids were actually less stable. It should be kept in mind that the changes observed during the course of these experiments are minor for the entire hybrid series. We focus here on the kinetic differences which, remarkably, show no clear relationship to the predicted colloidal stability of the micelles, and a high tolerance toward changes in the solvent conditions.

It should be recalled that the hybrid micelle experiments described above employ two copolymers of unequal PCL block lengths. Thus, both the corona composition and the average core block length change at the same time. As we discussed in a previous article, the morphological stability of PEO-*b*-PCL spheres in water improves as the PCL block length is increased.[57] Given the negligible effects of pH and salt additives on the PAA_{57}-*b*-PCL_{47} spheres, and in light of our prior findings, it is more likely that the stability trends of the hybrids are related to the core block size than to the composition of the corona. Note that the latter relationship also contradicts the classical stability expectations for core–shell colloids, whereby smaller core-to-shell size ratios should actually improve stability. Instead, shorter PCL blocks are associated with smaller micelle diameters and, thus, more severe crystal confinement. In turn, morphological rearrangements may permit these systems to alleviate the confinement penalty.

Inspired by the results of our preliminary work on the PEO-*b*-PCL system,[54] we expected that coassembly with homo-PCL additives, under the appropriate conditions, could also endow the PAA-*b*-PCL spheres with the capacity to self-assemble hierarchically into well-defined crystalline products. The final structure, inaccessible without the homo-PCL, should form passively during sample storage (for roughly 1 day), as if the additive chains were encoding instructions for the spheres to come together and create new structures at a later time. We noted previously that the average product shapes and sizes are additive dose-dependent. For the present study, however, we examined samples of fixed homopolymer content to evaluate what types of structures are formed when the composition of the hydrophilic corona is varied. In particular, we introduced the additive PCL_{10}, shown earlier to be morphogenically active, to the hybrid micelle samples at a fixed amount (equal to 10% of the total block copolymer weight). After ensuring that the initial comicellization product was spherical, we then characterized the transformation products which appeared over time.

We first sought to determine whether the single-component PAA_{57}-*b*-PCL_{47} spheres, having shown no signs of morphological evolution in the homopolymer-free experiments, would be influenced at all by the added PCL_{10} chains in the micelle core. Figure 2A presents TEM images of the transformation products obtained from PAA_{57}-*b*-PCL_{47} spheres that contain

chains of PCL_{10}, thereby confirming its morphogenic effect (supporting light scattering data are shown in Supporting Information Figure SI-3). As the TEM images suggest, coassembly with PCL_{10} favors a transition from spheres to micrometer-sized lamellae; these products bear sharp edges and exhibit a lozenge-like shape (see Supporting Information Figure SI-4 for additional images). Conversely, the lamellar products imaged in PCL_{10}-containing samples of PEO-*b*-PCL are elongated and fringed at opposing short edges; a representative TEM image of fringed PEO_{45}-*b*-PCL_{24} lamellae (termed "rafts") is provided in Figure 2B for comparison. The latter samples also contain significant amounts of free rod micelles, which are rare in homopolymer-containing PAA-*b*-PCL samples. We could not confirm whether either of these systems, if given sufficient time to evolve, would convert quantitatively into lamellae; the associated challenge would be the gradual degradation of PCL, a biodegradable polyester which is prone to hydrolysis over time. For PEO-*b*-PCL, the initial spherical micelles are eventually consumed, but the same was not confirmed in the PAA-*b*-PCL system. Inasmuch as our data reflects a late, although perhaps not final, stage of the transition, lamellae coexist with rods and with spheres for the PEO-*b*-PCL and PAA-*b*-PCL systems, respectively. These differences are consistent with the hypothesis that PEO-*b*-PCL "rafts" are built from rod-like subunits, while sharp-edged lamellae such as those shown in Figure 2A may involve a direct sphere-to-lamella transition. In sum, for both copolymer types, the use of PCL_{10} leads to the formation of large lamellae that are reminiscent of single-crystalline platelets; however, the preferred lamella formation pathway changes as the corona is altered, in turn affecting the lamellar shape.

The next experiments probe how the ionization state of the PAA corona might affect the product morphology. First, to ensure the presence of negative charges in the corona, a molar excess of CsOH base was added just after the initial spheres were formed, and the samples were then dialyzed against pure water; a relatively mild procedure was needed here to avoid base hydrolysis of the PCL block and, thus, a total conversion of the PAA into its salt form is not actually expected. Conveniently, the CsOH base also serves as an electron-dense counterion of PAA, providing contrast to these otherwise poorly visible structures in TEM images; typical results are presented in Figure 2C, where both micrometer-sized lamellar products and, at higher magnification, spherical micelles can be visualized simultaneously. These stain-enhanced images suggest that the Cs^+ counterion had remained with the PAA chains even after dialysis and, therefore, indicate that the PAA had been carrying a negative charge all along. The resulting lamellar products, as observed by TEM, are very similar to those shown in Figure 2A, most likely because the PAA block is also charged in pure water.

To convert most of the PAA into its neutral acid form, the experiment was performed instead at an acidic pH of 2.5. As in the previous example, the solution conditions were altered while the system was still in the form of spheres; these spheres were then left to transform at the adjusted pH value. As mentioned above in connection to the homopolymer-free experiments, because like-charged micelles are mutually repulsive, neutralizing the PAA corona should facilitate aggregation processes, which in turn might promote lamellar growth. It is also worth noting that the hydrated configuration of the PAA chains is expected to change significantly upon neutralization. Polyelectrolyte chains tend to adopt extended configurations due to local electrostatic repulsion; once this repulsion becomes negligible, the chains may adopt a more compact configuration. Thus, in regard to their chain configuration in the corona, neutralized PAA chains would resemble PEO. TEM images of the lamellar products obtained under acidic conditions are shown in Figure 2D. These lamellae appear rugged at two opposing edges, where there seems to be slower growth or growth interference as compared to the lozenge-shaped lamellae obtained at higher pH values. The PAA corona, therefore, affects the self-assembly process differently depending on its ionization state. The acid form in particular seems to have an inhibitory effect on lamellar growth, perhaps through a "poisoning" mechanism involving its transient adsorption onto the crystalline edges, similar to that observed in other systems.[58,59]

Having first seen how each copolymer system alone is influenced by the PCL_{10} chains, we then focused on the hybrid micelles. Figure 3A shows TEM images of the transformation products formed from hybrid spheres of PEO_{45}-*b*-PCL_{24} and PAA_{57}-*b*-PCL_{47} that contain PCL_{10} homopolymer in the core. The transformation products are lamellar, they bear no rod-like fringes, and are lozenge-shaped, just like the aggregates described above (see Figure 2A,B). Curiously, therefore, the shape is not altered by the presence of PEO_{45}-*b*-PCL_{24}, as no composition-dependent trends were identified for the hybrid samples. Because the polydispersity in size for these lamellae is greater than for the PEO-*b*-PCL "rafts" we described previously, we hesitate to quantify lamella formation rates here using light scattering data, although fewer products were actually found by TEM at increased PAA_{57}-*b*-PCL_{47} fractions. These results suggest a possible kinetic effect due to the composition of the hybrid, whereas the morphology, conversely, remains unchanged. It appears that relatively small proportions of PAA in the corona (as low as 20% w/w) lead to a complete, and unexpected, dominance of the self-assembly pathway associated with the PAA_{57}-*b*-PCL_{47} system over the "raft"-type lamella formation displayed by PEO_{45}-*b*-PCL_{24}.

To ascertain whether the lamellar shape preference involves some form of demixing between the two

block copolymer types, we prepared spheres using a *bis*-hydrophilic triblock copolymer (PEO_{45}-*b*-PCL_{37}-*b*-PAA_{72}) for which both hydrophilic chains are part of the same macromolecule. Polymer synthesis was performed according to procedures described in an earlier study.[60] Just as for the hybrid samples described above, PCL_{10} was used to induce lamella formation in water from spheres prepared using the triblock copolymer. As evidenced by the TEM images in Figure 3B, the system once again yields sharp-edged products, and not the fringed "raft"-type lamellae. A second remarkable feature associated with these triblock samples is the distinctly elevated hydrophilic content as compared to all other samples considered in this work (as summarized in Table SI-1 in the Supporting Information). The PCL weight fraction of the triblock alone is 0.37, which increases to an effective value of 0.43 when accounting for the added weight of the PCL_{10} in the core; the micelles are mostly hydrophilic in composition, yet they still evolve to produce lamellae.

Beyond the fact that the lamellar morphology is more commonly associated with "crew-cut" block copolymers than the relatively hydrophilic materials which were employed here, we also highlight an unusual preference in our samples for large open sheets rather than closed vesicles. The bilayer-forming composition range of PEO-*b*-PCL in water, for example, has been the subject of several studies.[31,61,62] This range encompasses materials that are much more PCL-rich than our homopolymer-containing samples, and is associated predominantly with vesicle formation. Furthermore, for all *bis*-hydrophilic micelles examined here, the presence of two different types and sizes of hydrophilic chains on a lamellar surface actually should allow for the system to stabilize curvature quite efficiently.[60,63] Despite the additional curvature stabilization mechanism made possible here, the transformation products are planar. While the lack of curvature observed here may be due to the crystalline nature of the PCL core, sufficiently rigid systems which are amorphous may also behave similarly, as demonstrated in recent work.[64]

Because the PCL_{10} chains are entirely hydrophobic, their transfer or release into water should be highly inefficient. The following tests examine the interplay between a set of homopolymer-containing spheres and a second micellar population that contains no homo-PCL. To this end, we mixed separate (preformed) micellar populations of PEO_{45}-*b*-PCL_{24} and PAA_{57}-*b*-PCL_{47}, and allowed them to coevolve in water; only one of the two micellar populations was made in the presence of PCL_{10}. As suggested by the TEM images in Figure 4A,B, the shape of the final products is the same in each case. These products are lamellar, oval-shaped and presenting rugged edges that are particularly obvious at the two opposing apexes. The different edge properties, the symmetry of the products, as well as our observation of some heart-shaped and, apparently, twinned lamellae are all features which suggest that the internal regions of crystalline PCL are likely to be aligned throughout these assemblies. When both micellar populations harbor the PCL_{10} chains, their coevolution results instead in much larger hexagonal lamellae that exhibit a distinctly less elongated profile. As shown in Figure 4C, the latter structures are also rugged, they contain no rod-like fringes, and are clearly unique in shape with respect to the lamellae shown in Figure 4A,B.

For all samples represented by Figure 4, it should be recalled that the block copolymers, unlike the PCL_{10} component, can exchange between micellar objects in water, to an extent that is limited by the critical micelle concentration. The formation of similar oval-shaped lamellae, regardless of which of the two micellar populations is carrying the PCL_{10} additive, might possibly indicate that some form of chain exchange was involved. However, the products shown in Figure 4 also differ with respect to the lozenge-shaped lamellae found in true hybrid samples (see Figure 3), where the two chain types are mixed deliberately during sample preparation. We suspect that the lamellae evolve through a particle-based growth mechanism primarily, which seems to occur differently in homogeneous samples than it does for coaggregating samples. As a secondary phenomenon, the molecular exchange between two separate micelle populations is also possible; however, this exchange process probably does not have a major influence over the shape of the lamellar products.

It is remarkable that none of the mixed samples yields the same type of products that would be observed for any of these additive-doped micellar populations alone. There were no signs of either the lozenge-shaped lamellae associated with PAA_{57}-*b*-PCL_{47}, or of the "rafts" formed with PEO_{45}-*b*-PCL_{24}. The formation of a third, unique lamellar type (Figure 4A,B) suggests that the additive-free micellar population does influence self-assembly. We also highlight that there were no rod micelles in the sample represented by Figure 4A: since rods are normally formed in samples of pure PEO_{45}-*b*-PCL_{24} (without PCL_{10}), their absence here suggests that the material, instead, participated in transformation processes related to the PAA_{57}-*b*-PCL_{47} spheres, which do contain homopolymer. Precisely how spheres of one material might be incorporated into growing crystals of the other material is not clear at present, but a mutual influence is apparent. Only three combinations were needed here in order to demonstrate the latter phenomenon, but a full phase map has the potential to reveal many unique morphological features. As compared to most other block copolymer aggregate morphologies, the fact that the primary structures, simple spherical aggregates, can be prepared with

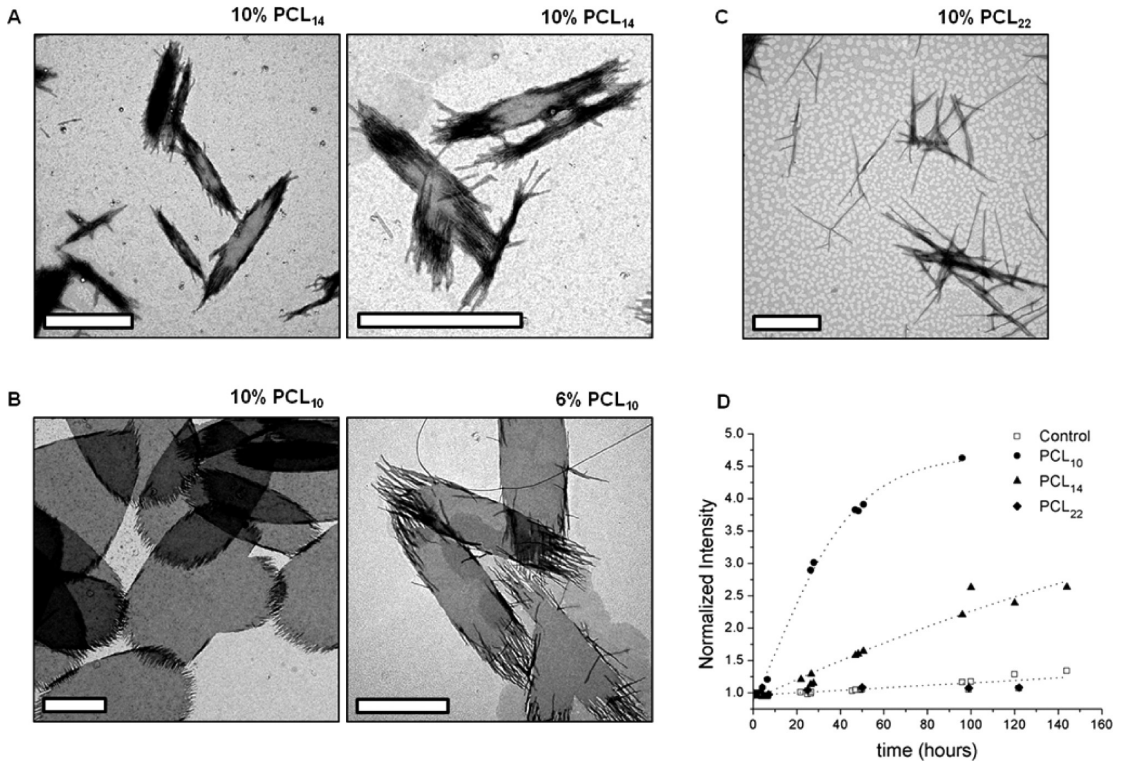

Figure 5. Chain-length dependence of the homopolymer effect. TEM images of "raft"-type lamellae found in samples of PEO_{45}-*b*-PCL_{24} containing (A) PCL_{14} and (B) PCL_{10} additives (content listed above each image). Note the larger size of the products shown in (B). For the samples corresponding to the right side image, an equimolar homo-PCL chain concentration is used with respect to the samples in (A), indicating an intrinsic difference in their activity. (C) TEM images of ribbon-like products obtained when using the inactive PCL_{22} additive. (D) Evolution of light scattering intensity with time for PEO_{45}-*b*-PCL_{24} samples containing 10% (w/w) homo-PCL (chain length indicated in legend). The kinetic trends corroborate the images shown in (A) and (B); note the similar profiles of PCL_{22}-containing and control micelles. Scale bar: 2 μm.

relative ease is also attractive from the standpoint of materials design.

Mechanistic Aspects of the Homopolymer Effect. So far, we described the effects of one highly active homo-PCL sample (PCL_{10}) on a range of block copolymer aggregate types. To generalize the strategy, it would be useful to establish a set of criteria relating specifically to the homo-PCL component. For testing purposes, PEO-*b*-PCL block copolymers were judged as being most suitable, since the morphological phase behavior of this material has been studied extensively.[31,61,62] Representative calorimetric data for the series of homopolymers used here and for homopolymer-containing block copolymer micelles are presented in Figures SI-5 and SI-6 in the Supporting Information, respectively. As reported previously, crystallinity values of approximately 65% are typical for the mixed PCL phase in freeze-dried micelles made of diblock and homopolymer mixtures.[54] In the latter work, although the PCL crystallization peak areas were found to increase in proportion to the amount of added PCL homopolymer, the increase in crystallinity was very subtle when normalized to the total PCL weight fraction. This feature of our test system suggests that the morphological behavior, which varies significantly with the homopolymer content, must involve factors other than the total degree of core crystallinity; these factors will be discussed further below. In addition, selected-area electron diffraction (SAED) patterns, obtained from the lamellar products, suggest that these nanostructures are indeed crystalline (see Supporting Information Figure SI-7). Height profiles obtained using atomic force microscopy are also shown in the Supporting Information (Figure SI-8).

The initial mechanistic tests used TEM and light scattering measurements to characterize PEO_{45}-*b*-PCL_{24} micelles that contain linear PCL chains of different lengths (at a constant weight fraction); representative data are shown in Figure 5. As can be surmised from these results, the longer homo-PCL chains are also less active. For instance, the use of PCL_{14} yields lamellar products that are distinctly smaller than those obtained with PCL_{10}; the changes also occur more slowly. To correct for differences related to the molar concentration, additional samples were prepared with appropriately reduced amounts of PCL_{10}. The products were, nevertheless, larger than those found in the PCL_{14}-containing micelles: a 4-fold average surface area difference was estimated based on TEM images (compare Figure 5, panels A and B, right side image); the same trends in average size are also apparent in solution based on DLS measurements (see Figure SI-9

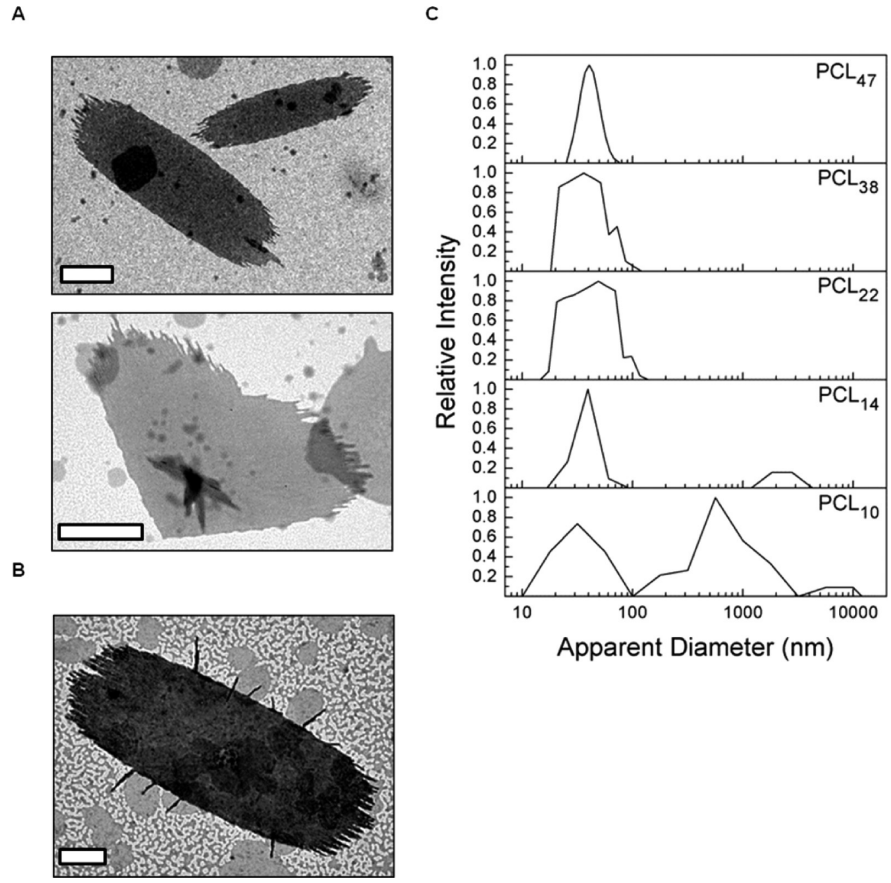

Figure 6. "Crew-cut" PEO-*b*-PCL block copolymers and the homopolymer effect. TEM images of "raft"-type lamellae and twinned lamellae observed in samples of (A) PEO_{45}-*b*-PCL_{66} and (B) PEO-rich PEO_{114}-*b*-PCL_{28}. Each sample contains 10% (w/w) PCL_{10}. (C) DLS data for PEO_{45}-*b*-PCL_{49} samples containing 10% (w/w) homo-PCL (chain length indicated in legend). A single broad diffusive population is found when using homo-PCL of 22 repeat units or more; large aggregates are detected in the samples containing shorter homo-PCL chains. DLS samples are isochronal. Scale bar: 2 μm.

in the Supporting Information). With a further increase of the homo-PCL length to 22 repeat units (which approaches the length of the core-forming block), the effects on morphology seem to disappear. When using PCL_{22}, the products ultimately found are ribbon-like and thus very similar to those found in control samples (Figure 5C and Supporting Information Figure SI-9). These results suggest that the activity decreases as the homo-PCL chain length increases. The effects, specifically, become negligible for additives above a cutoff chain length value somewhere between 14 and 22 repeat units.

Through further tests, we confirmed that the cutoff value correlates with the absolute homo-PCL chain length, and not the chain length ratio between the additive and the core-forming block. This ratio is important when the micelles are formed initially, but it is not later relevant to the morphology, provided that the additive can be incorporated properly during self-assembly.[65] To illustrate this point, the experiments were repeated using PEO-*b*-PCL copolymers of increased core block length; selected TEM images are provided in Figure 6A. In the case of PEO_{45}-*b*-PCL_{49}, for instance, time-dependent changes were observed for the micelles containing the same short-chain PCL_{10} and PCL_{14} additives, as suggested by the DLS results shown in Figure 6C. No effects, however, were found for any of the longer additives which were examined. The latter samples remain unchanged from their initial state as spherical micelles. We reproduced the same chain length cutoff for the homopolymer effect in the PAA-*b*-PCL system (see Figure SI-10 in the Supporting Information). It is worth noting, as well, that all of the PEO-*b*-PCL copolymers we tested yield "raft"-type lamellae as a result of PCL_{10} incorporation. To showcase the similarity of the products, along with the images of lamellae we obtained from PCL-rich "crew-cut" block copolymers, we provide in Figure 6B an image taken from a PEO-rich sample (PEO_{114}-*b*-PCL_{28}) that also yields "rafts". The morphological behavior, therefore, seems to be remarkably insensitive to the composition of the diblock, which showcases the versatility associated with this self-assembly strategy. The transformation process, in addition, is thermally reversible, such that heating the "rafts" to temperatures which melt the PCL transforms the lamellae back into spheres; if these spheres are then stored at cooler temperatures, such that the core may recrystallize, the

"rafts" are formed once again (see Figure SI-11 in the Supporting Information).

To distinguish the importance of molecular weight from that of chain length, we performed control experiments in which the linear additives were replaced by 3-arm star homo-PCL. These branched macromolecules should have the same solubility profiles as their linear counterparts, but they are distinctly less crystalline. As expected, the branched additives were much less effective at driving morphological changes than the linear homo-PCL (see Figures SI-12 and SI-13 in the Supporting Information). Some of the low molecular weight branched homo-PCL we used are amorphous at ambient temperature and exist in the form of clear, viscous liquids; these amorphous additives have no noticeable effects on the micelle morphology. Thus, it is the homopolymer chain length, and not the molecular weight, that is relevant to the morphological effects, and the crystallinity of the additive, moreover, seems to be a crucial factor.

In trying to explain chain length cutoff value, we take inspiration from the fact that a similar value has been reported for another phenomenon involving the crystallinity of PCL chains. In bulk studies, fractional crystallization was also found to obey a distinct chain-length cutoff, such that chains which are incapable of spanning the thickness of a crystalline lamella are rejected to the outer crystal edges.[66] Using exceptionally low-polydispersity PCL samples, a critical thickness value of ~12.9 nm was reported, which corresponds to 15−17 repeat units of PCL in its crystalline conformation; chains of a size equal to or lower than this value tend not to partake in chain-folded crystallization and, instead, fractionate. For micelles, the same selection criteria should apply in deciding the miscibility between the PCL homopolymers and the PCL blocks within the crystalline subphase of the core. Thus, the onset of chain-folding depends on the length of the crystallizing polymeric chains which, in turn, may provide a relevant length scale in order to duplicate these effects in other block copolymer systems.

The hypothesized consequence of fractionation inside of the micelles is depicted in Scheme 2, where we illustrate the preferred localization within the micelle core of homo-PCL chains, both above and below the chain length cutoff. Amphiphilic block copolymers (color coding is blue for PEO, red for PCL) can solubilize homopolymer chains of different lengths (red with black outline). Upon micellization, when the core is amorphous, these structures are virtually identical. In the schematic examples shown, the PCL block, which makes up most of the core volume, is folded within the crystal phase. Sufficiently large homo-PCL chains are expected to show no particular preference, and distribute themselves uniformly within the core; we represent the latter

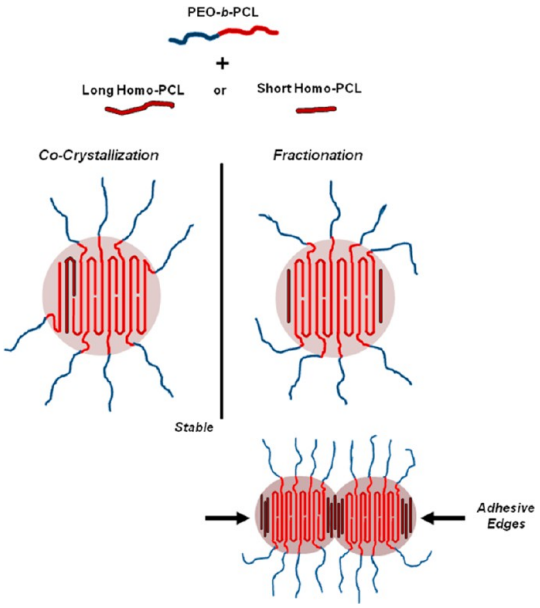

Scheme 2. Homopolymer Distribution within a Crystallized PCL Micelle Core

scenario by showing a homo-PCL chain embedded within the crystalline region of the core (left side). Conversely, PCL oligomers should not have easy access to the central part of that crystalline region, unless a crystal defect is incurred. Instead, the shorter chains would tend to crystallize at the edges of a pre-existing crystal, composed of the longer core-forming PCL blocks (right side). In principle, as long as the supply of amorphous PCL blocks remains high, the crystallization of the homo-PCL oligomers will be disfavored. Thus, only when crystal growth has slowed down considerably could these oligomers, which had been rejected from crystallizing so far, finally compete with the PCL blocks. As a result, the homo-PCL would accumulate near the surface of the core and, in extending the crystalline PCL region, it may facilitate the exposure of crystal edges to the aqueous surroundings. It should be recalled that the homopolymer chains provide no stability against intermicellar aggregation, as only the block copolymer chains contribute toward forming the hydrophilic corona. Thus, homopolymer-enriched crystal edges may be stabilized less effectively by the soluble corona-forming chains, as the homopolymer itself contains no such chains. We propose that, in this manner, expelled homopolymer chains render the micelles mutually adhesive, while obeying an anisotropic directionality that is derived from the PCL crystal.

CONCLUSIONS

A simple and versatile self-assembly approach is described, whereby coassembled structures made from semicrystalline block copolymer and homopolymer chains transform spontaneously into hierarchical crystalline products directly in water. This

results in lamellar assemblies that are reminiscent of block copolymer single crystals, while being very different in regard to the formation mechanism. Versatility is demonstrated through the range of micelle types that can be manipulated by using homo-PCL. These heterogeneous systems are candidates for further organization, for example, in the form surface or core patterning. Other than PEO-*b*-PCL, crystallinity-related aspects have not been examined before for any of the materials on which we report here. Due to the hydrophobic nature of the PCL block, these would all be particularly challenging materials from which to grow large crystals in water, yet this is achieved here in a controllable manner.

On a basic level, all of the systems investigated in this work produce lamellae in the presence of homo-PCL, and thus display convergent behavior. Nevertheless, several important differences were found when comparing the lamellae, which show that the long-range features are potentially addressable. In the first part of the manuscript, we describe shape variations that depend on the soluble block chemistry. Homopolymer-containing PEO-*b*-PCL samples yield lamellae that are elongated and fringed, while PAA-stabilized samples produce lozenge-shaped lamellae with sharp edges. As the PAA block is ionizable, pH changes also affect the lamellar properties. Smaller structures and slower kinetics are observed under acidic conditions, which favor charge neutralization; the results thus contradict classical expectations based on the corona chain repulsion, in which case such micelles should be less stable at low pH, which was not observed. For hybrid micelles containing both PEO and PAA, the lozenge-like structures prevail throughout the entire composition range that was examined. These structures appear similar, but present very different surface properties. If, instead, the same two copolymers are employed as separate micelle populations, which are then allowed to coevolve in water, different lamellar shapes are obtained. Such subtle procedural variations affect the outcome significantly, and thus offer added flexibility in structure design.

To appreciate the mechanism behind the homopolymer effect, a screening of homo-PCL additives is described in the final part of the manuscript. The morphogenic activity shows a distinct correlation with the additive chain length, and homopolymer crystallinity is also prerequisite. Specifically, the length dependence is manifested as a cutoff in activity somewhere between 14 and 22 PCL repeat units. This value is believed to be linked to the average PCL crystal thickness, and to a type of fractional PCL crystallization within the micelle core which, ultimately, coordinates the association of smaller micellar entities to create an extended lamellar crystal. The emergence of the new lamellar morphology is thus crystallinity-driven, which involves both the homo-PCL and the PCL blocks, but may be kinetically inaccessible without the homopolymer chains.

EXPERIMENTAL SECTION

Materials. Poly(ethylene oxide) monomethyl ether (number average molecular weights, M_n 2000 and 5000 g mol^{-1}), ε-caprolactone (CL, 99%), *tert*-butyl acrylate (tBA), 2-bromoisobutyryl bromide (98%), allyl alcohol (anhydrous, >99%), benzyl alcohol (anhydrous, >99%), copper(I) bromide (CuBr), *N*,*N*,*N*′,*N*′,*N*″-pentamethyldiethylenetriamine (PMDETA, 99%), trimethylsilyl iodide ((TMS)I), tin(II)-2-ethylhexanoate ($SnOct_2$, 95%), phosphotungstic acid, cesium hydroxide solution (50 wt % in H2O), 1,1,1-tris(hydroxymethyl)propane (TMP) and polycaprolactone triol (M_n 300 and 900 g mol-1) were obtained from Aldrich (Oakville ON, Canada). The monomers, CL and tBA, were dried over CaH_2 for 2 days and distilled under reduced pressure before use; the tBA was passed through a column of MEHQ inhibitor remover before adding the CaH_2. PMDETA was dried and distilled similarly, but stored at −20 °C; before use, N_2 was bubbled through the ligand for 15 min as a preliminary deoxygenation step. The PEO macroinitiator was dried by azeotropic distillation in toluene. CuBr was kept in excess glacial acetic acid overnight, filtered and then washed with copious amounts of absolute ethanol, followed by anhydrous ethyl ether. The purified CuBr was vacuum-dried at 80 °C for 3 days, and stored under N_2 at 4 °C. All other chemicals and solvents were used as received.

Polymer Synthesis. Block copolymers of PEO-*b*-PCL were prepared by ring-opening polymerization, using a monofunctional PEO as the initiating species, in the presence of $SnOct_2$ catalyst, following Bogdanov *et al.*[67] In summary, a known amount of PEO was dissolved in toluene and dried by azeotropic distillation while under a N_2 atmosphere. The appropriate amount of CL was then added, followed by the $SnOct_2$ catalyst (*ca.* 0.05 equiv relative to hydroxyl groups), which was dissolved first in a minimal amount of dry toluene. The reaction mixture was then heated gradually to 130 °C and stirred overnight at the latter temperature. The product was then isolated initially by precipitation in a large excess of hexanes, and then precipitated once more either in ethyl ether or in isopropyl alcohol (with subsequent storage at −20 °C for 2 days). The two procedures gave indistinguishable results. The homopolymer samples were prepared in a similar manner using anhydrous small molecule initiators. The linear homopolymers were initiated either with allyl or benzyl alcohol; branched samples were prepared using the trifunctional TMP initiator.

The PAA-*b*-PCL copolymers were prepared through controlled radical polymerization starting with a PCL homopolymer as the macroinitiator, prepared as described above. The PCL hydroxyl terminus first was made capable of initiating radical polymerization by acylation with 2-bromoisobutyryl bromide; the end-modified PCL was isolated and then purified in the same fashion as described above. Next, the macroinitiator, tBA monomer, CuBr and PMDETA ligand (1.5 equiv with respect to macroinitiator) were dissolved in toluene and deoxygenated by multiple freeze−thaw cycles. The reaction mixture was then heated to 110 °C and left stirring for 6 h in an N_2 atmosphere. The PMDETA−CuBr complex was then removed with the aid of an activated alumina column, and the eluate was precipitated in hexanes. To convert the PtBA block into PAA, the butyl ester deprotection was performed by adding a slight molar excess of TMS(I) to a solution of the product in chloroform at ambient temperature. The solvents were then evaporated, and the product was added, as a minimal solution in THF, to an excess of acidified 10 g/L aqueous sodium metabisulfite. The salts were removed by dialysis against Milli-Q water, and the PCL-*b*-PAA

product was isolated by freeze-drying. The triblock copolymer samples were prepared similarly, using a PEO-*b*-PCL copolymer as the macroinitiator.

Polymer Characterization. The degrees of polymerization and polydispersity indices of the polymers were assessed through gel permeation chromatography (GPC) experiments performed in THF, using a Waters 510 liquid chromatography pump equipped with 2 Styragel columns connected in series (HR1 and HR4). A Varian RI-4 refractive index detector was used for GPC. The calibration was performed using polystyrene standards of a narrow molecular weight distribution (Scientific Polymer Products, Inc., NY). NMR spectra were recorded on a Varian XL-300 spectrometer using tetramethylsilane as the internal reference. The relative number average degrees of polymerization (DP) of each block were obtained by comparing the integrated ^{1}H NMR peak areas corresponding to PEO (3.6 ppm), PCL (4.1 ppm) and, as applicable, to the acrylate backbone of the PtBA and PAA blocks (2.3 ppm). The absolute DP values were estimated from the relative DP and the supplier-specified DP value of PEO; the values thereby obtained were corroborated both by GPC and end-group analysis by ^{1}H NMR.

Micelle Preparation. The block copolymers were first dissolved in dioxane or DMF at a concentration of 5 g/L (the results were equivalent when using either solvent). Next, 5 vol of Milli-Q water was added, under stirring, at an adjusted constant rate over a period of 5 min. The average diameter and size distribution of these initially formed micelles was verified by DLS. The residual solvent was then removed by dialysis against Milli-Q water (dialysis tubing: MEMBRA-CEL MD34-14, 14 000 g/mol cutoff) for a period of 1 day. Upon re-evaluation by DLS, the micelles were then filtered using 0.45 μm cutoff Supor Syringe filters (Pall Corporation, NY) prior to characterization if large-sized aggregates were not detected. The filtration step was performed before dialysis instead, when necessary, to avoid the removal of transformation products.

For homopolymer-containing micelles, the desired volume of homopolymer solution (5 g/L in dioxane or DMF) was introduced to the sample prior to micelle formation by the addition of water. The nominal block copolymer concentration of the micellar samples prepared in this fashion is 0.83 g/L. The homopolymer content of the micelles is expressed as a weight percentage with respect to the latter value. For the pH-dependent experiments, when specified, an aliquot of 50 wt % CsOH solution in water was added to the micelles, just prior to the dialysis step, to achieve a 20 mM concentration; at the latter concentration, the CsOH is no less than 4 equiv with respect to the PAA repeat units. The acidified samples were adjusted to a nominal pH value of 2.5 using a standardized 0.1 M hydrochloric acid solution in water; as verified using DLS, the acid was introduced prior to any changes in the sample size distribution.

Transmission Electron Microscopy (TEM). For TEM sampling, the micellar solutions were first diluted to a concentration of 0.2 g/L and then stained with an equal volume of phosphotungstic acid at a concentration of 1 g/L in water. For each of these diluted and stained samples, an aliquot of 5 μL was deposited onto a copper grid coated either with carbon or a Formvar-supported carbon film (Electron Microscopy Science, Hatfield, PA) and allowed to air-dry. The images were taken on a JEOL 2000FX microscope operating at a voltage of 120 kV.

Light Scattering. Dynamic light scattering (DLS) measurements were performed on a Brookhaven BI-200SM goniometer, equipped with a BI-9000AT digital correlator and a Compass 315M-150 laser (Coherent Technologies, TX), which was used at a wavelength of 532 nm. Autocorrelation functions were analyzed using the CONTIN algorithm. All acquisitions were made at room temperature. Regarding kinetic experiments, it is significant that the sample size distribution changes occurred on a far longer time scale (hours or days) than any single acquisition (typically 360 s). Thus, size distributions could be obtained as a function of time, and the average photon count rate could be used to monitor increases in the scattered light intensity with time, provided that the instrument optics are kept constant.

Differential Scanning Calorimetry. The measurements were performed on a Q2000 DSC instrument (TA Instruments, DE) with aluminum pans. Each heat−cool−heat experiment was performed, starting at the idle instrument temperature of 40 °C, in the range from 5 to 80 °C at heating/cooling rates of 5 °C/min. Data from the first heating process were not used. Solid samples were loaded directly onto the pans; micellar samples were first flash-frozen with liquid N_2 and then freeze-dried to obtain a powder for characterization. Data analysis was performed using Universal Analysis version 3.9A software. Crystallinity values were calculated from the crystallization peaks (cooling cycle), taking 15.4 kJ/mol as the theoretical heat of fusion of 100% crystalline PCL. Peak areas were corrected for the total PCL weight fraction in each case, accounting for the block and homopolymer weights as appropriate.

Atomic Force Microscopy. The samples were prepared by drop-casting onto freshly cleaved mica, and allowing to dry overnight. Imaging was performed on a MultiMode SPM connected to a Nanoscope controller (Digital Instruments, Veeco Metrology Group, CA) using the ScanAsyst mode, with a scan rate of 1 Hz.

Conflict of Interest: The authors declare no competing financial interest.

Supporting Information Available: Further details on the molecular characteristics of the polymers and on the composition of the micellar samples are provided, in addition to supporting DLS data, TEM and AFM images, calorimetric data, and SAED data, as referred to throughout the manuscript. This material is available free of charge *via* the Internet at http://pubs.acs.org.

Acknowledgment. The authors thank the Fonds Québécois de la Recherche sur la Nature et les Technologies (FQRNT), the Centre for Self-Assembled Chemical Structures (CSACS), and the National Sciences and Engineering Research Council of Canada (NSERC) Discovery grant for financial support. Thanks are also due to Dr. Tony Azzam for preparing several of the materials in connection with earlier work (specifically: homopolymer samples PCL_{38} and PCL_{47}, and diblock copolymers PEO_{45}-*b*-PCL_{18} and PEO_{45}-*b*-PCL_{66}) and to Dr. Karina M. M. Carneiro for performing the AFM analyses.

REFERENCES AND NOTES

1. Hawker, C. J.; Russell, T. P. Block Copolymer Lithography: Merging "Bottom-Up" with "Top-Down" Processes. *MRS Bull.* **2005**, *30*, 952–966.
2. Liu, G.; Wyman, I. Architectural Polymers, Nanostructures, and Hierarchical Structures from Block Copolymers. In *Complex Macromolecular Architectures: Synthesis, Characterization, and Self-Assembly*; Hadjichristidis, N.; Hirao, A.; Tezuka, Y.; Du Prez, F., Eds.; Wiley: Singapore, 2011; pp 739−761.
3. Elsabahy, M.; Wooley, K. L. Design of Polymeric Nanoparticles for Biomedical Delivery Applications. *Chem. Soc. Rev.* **2012**, *41*, 2545–2561.
4. Li, B.; Li, C. Y. Immobilizing Au Nanoparticles with Polymeric Single Crystals, Patterning and Asymmetric Functionalization. *J. Am. Chem. Soc.* **2007**, *129*, 12–13.
5. Nie, Z.; Fava, D.; Kumacheva, E.; Zou, S.; Walker, G. C.; Rubinstein, M. Self-Assembly of Metal-Polymer Analogues of Amphiphilic Triblock Copolymers. *Nat. Mater.* **2007**, *6*, 609–614.
6. Nardin, C.; Widmer, J.; Winterhalter, M.; Meier, W. Amphiphilic Block Copolymer Nanocontainers as Bioreactors. *Eur. Phys. J. E* **2001**, *4*, 403–410.
7. Palivan, C. G.; Fischer-Onaca, O.; Delcea, M.; Itel, F.; Meier, W. Protein-Polymer Nanoreactors for Medical Applications. *Chem. Soc. Rev.* **2012**, *41*, 2800–2823.
8. Carneiro, K. M.; Aldaye, F. A.; Sleiman, H. F. Long-Range Assembly of DNA into Nanofibers and Highly Ordered Networks Using a Block Copolymer Approach. *J. Am. Chem. Soc.* **2010**, *132*, 679–685.
9. Bates, F. S.; Hillmyer, M. A.; Lodge, T. P.; Bates, C. M.; Delaney, K. T.; Fredrickson, G. H. Multiblock Polymers: Panacea or Pandora's Box? *Science* **2012**, *336*, 434–440.
10. Zhu, J.; Zhang, S.; Zhang, K.; Wang, X.; Mays, J. W.; Wooley, K. L.; Pochan, D. J. Disk-Cylinder and Disk-Sphere

Nanoparticles *via* a Block Copolymer Blend Solution Construction. *Nat. Commun.* **2013**, *4*, 2297.
11. Christian, D. A.; Tian, A. W.; Ellenbroek, W. G.; Levental, I.; Rajagopal, K.; Janmey, P. A.; Liu, A. J.; Baumgart, T.; Discher, D. E. Spotted Vesicles, Striped Micelles and Janus Assemblies Induced by Ligand Binding. *Nat. Mater.* **2009**, *8*, 843–849.
12. Li, Z. B.; Hillmyer, M. A.; Lodge, T. P. Morphologies of Multicompartment Micelles formed by ABC Miktoarm Star Terpolymers. *Langmuir* **2006**, *22*, 9409–9417.
13. Groschel, A. H.; Schacher, F. H.; Schmalz, H.; Borisov, O. V.; Zhulina, E. B.; Walther, A.; Muller, A. H. Precise Hierarchical Self-Assembly of Multicompartment Micelles. *Nat. Commun.* **2012**, *3*, 710.
14. Dupont, J.; Liu, G.; Niihara, K.; Kimoto, R.; Jinnai, H. Self-Assembled ABC Triblock Copolymer Double and Triple Helices. *Angew. Chem., Int. Ed.* **2009**, *48*, 6144–6147.
15. Randolph, L. M.; Chien, M.-P.; Gianneschi, N. C. Biological Stimuli and Biomolecules in the Assembly and Manipulation of Nanoscale Polymeric Particles. *Chem. Sci.* **2012**, *3*, 1363.
16. Eloi, J. C.; Rider, D. A.; Cambridge, G.; Whittell, G. R.; Winnik, M. A.; Manners, I. Stimulus-Responsive Self-Assembly: Reversible, Redox-Controlled Micellization of Polyferrocenylsilane Diblock Copolymers. *J. Am. Chem. Soc.* **2011**, *133*, 8903–8913.
17. Yu, S. Y.; Azzam, T.; Rouiller, I.; Eisenberg, A. "Breathing" Vesicles. *J. Am. Chem. Soc.* **2009**, *131*, 10557–10566.
18. He, Y.; Lodge, T. P. The Micellar Shuttle: Thermoreversible, Intact Transfer of Block Copolymer Micelles between an Ionic Liquid and Water. *J. Am. Chem. Soc.* **2006**, *128*, 12666–12667.
19. Cui, H.; Chen, Z.; Zhong, S.; Wooley, K. L.; Pochan, D. J. Block Copolymer Assembly *via* Kinetic Control. *Science* **2007**, *317*, 647–650.
20. Schmelz, J.; Karg, M.; Hellweg, T.; Schmalz, H. General Pathway toward Crystalline-Core Micelles with Tunable Morphology and Corona Segregation. *ACS Nano* **2011**, *5*, 9523–9534.
21. Wang, X.; Guerin, G.; Wang, H.; Wang, Y.; Manners, I.; Winnik, M. A. Cylindrical Block Copolymer Micelles and Co-Micelles of Controlled Length and Architecture. *Science* **2007**, *317*, 644–647.
22. Gadt, T.; Ieong, N. S.; Cambridge, G.; Winnik, M. A.; Manners, I. Complex and Hierarchical Micelle Architectures from Diblock Copolymers using Living, Crystallization-Driven Polymerizations. *Nat. Mater.* **2009**, *8*, 144–150.
23. Rupar, P. A.; Chabanne, L.; Winnik, M. A.; Manners, I. Non-Centrosymmetric Cylindrical Micelles by Unidirectional Growth. *Science* **2012**, *337*, 559–562.
24. Mihut, A. M.; Crassous, J. J.; Schmalz, H.; Drechsler, M.; Ballauff, M. Self-Assembly of Crystalline–Coil Diblock Copolymers in Solution: Experimental Phase Map. *Soft Matter* **2012**, *8*, 3163–3173.
25. Petzetakis, N.; Dove, A. P.; O'Reilly, R. K. Cylindrical Micelles from the Living Crystallization-Driven Self-Assembly of Poly(lactide)-Containing Block Copolymers. *Chem. Sci.* **2011**, *2*, 955–960.
26. Schmelz, J.; Schedl, A. E.; Steinlein, C.; Manners, I.; Schmalz, H. Length Control and Block-Type Architectures in Worm-like Micelles with Polyethylene Cores. *J. Am. Chem. Soc.* **2012**, *134*, 14217–14225.
27. Crassous, J. J.; Schurtenberger, P.; Ballauff, M.; Mihut, A. M. Design of Block Copolymer Micelles *via* Crystallization. *Polymer* **2015**, 10.1016/j.polymer.2015.02.030.
28. Su, M.; Huang, H.; Ma, X.; Wang, Q.; Su, Z. Poly(2-vinylpyridine)-block-Poly(caprolactone) Single Crystals in Micellar Solution. *Macromol. Rapid Commun.* **2013**, *34*, 1067–1071.
29. Wang, J.; Zhu, W.; Peng, B.; Chen, Y. A Facile Way to prepare Crystalline Platelets of Block Copolymers by Crystallization-Driven Self-Assembly. *Polymer* **2013**, *54*, 6760–6767.
30. Cao, L.; Manners, I.; Winnik, M. A. Influence of the Interplay of Crystallization and Chain Stretching on Micellar Morphologies: Solution Self-Assembly of Coil-Crystalline Poly(isoprene-*block*-ferrocenylsilane). *Macromolecules* **2002**, *35*, 8258–8260.
31. Rajagopal, K.; Mahmud, A.; Christian, D. A.; Pajerowski, J. D.; Brown, A. E.; Loverde, S. M.; Discher, D. E. Curvature-Coupled Hydration of Semicrystalline Polymer Amphiphiles yields Flexible Worm Micelles but favors Rigid Vesicles: Polycaprolactone-Based Block Copolymers. *Macromolecules* **2010**, *43*, 9736–9746.
32. Du, Z. X.; Xu, J. T.; Fan, Z. Q. Micellar Morphologies of Poly(epsilon-caprolactone)-*b*-Poly(ethylene oxide) Block Copolymers in Water with a Crystalline Core. *Macromolecules* **2007**, *40*, 7633–7637.
33. Zhang, J.; Wang, L. Q.; Wang, H.; Tu, K. Micellization Phenomena of Amphiphilic Block Copolymers based on Methoxy Poly(ethylene glycol) and either Crystalline or Amorphous Poly(caprolactone-*b*-lactide). *Biomacromolecules* **2006**, *7*, 2492–2500.
34. Gast, A. P.; Vinson, P. K.; Coganfarinas, K. A. An Intriguing Morphology in Crystallizable Block Copolymers. *Macromolecules* **1993**, *26*, 1774–1776.
35. Xu, J. T.; Fairclough, J. P. A.; Mai, S. M.; Ryan, A. J. The Effect of Architecture on the Morphology and Crystallization of Oxyethylene/Oxybutylene Block Copolymers from Micelles in *n*-Hexane. *J. Mater. Chem.* **2003**, *13*, 2740–2748.
36. Mihut, A. M.; Chiche, A.; Drechsler, M.; Schmalz, H.; Di Cola, E.; Krausch, G.; Ballauff, M. Crystallization-Induced Switching of the Morphology of Poly(ethylene oxide)-*block*-Polybutadiene Micelles. *Soft Matter* **2009**, *5*, 208–213.
37. Mihut, A. M.; Crassous, J. J.; Schmalz, H.; Ballauff, M. Crystallization-Induced Aggregation of Block Copolymer Micelles: Influence of Crystallization Kinetics on Morphology. *Colloid Polym. Sci.* **2010**, *288*, 573–578.
38. Xu, A. W.; Ma, Y. R.; Colfen, H. Biomimetic Mineralization. *J. Mater. Chem.* **2007**, *17*, 415–449.
39. Banfield, J. F.; Welch, S. A.; Zhang, H.; Ebert, T. T.; Penn, R. L. Aggregation-Based Crystal Growth and Microstructure Development in Natural Iron Oxyhydroxide Biomineralization Products. *Science* **2000**, *289*, 751–754.
40. Sleytr, U. B.; Messner, P.; Pum, D.; Sara, M. Crystalline Bacterial Cell Surface Layers (S Layers): From Supramolecular Cell Structure to Biomimetics and Nanotechnology. *Angew. Chem., Int. Ed.* **1999**, *38*, 1034–1054.
41. Kotov, N. A.; Srivastava, S. Nanoparticle Assembly for 1D and 2D Ordered Structures. *Soft Matter* **2009**, *5*, 1146–1156.
42. Khanna, K.; Varshney, S.; Kakkar, A. Miktoarm Star Polymers: Advances in Synthesis, Self-Assembly, and Applications. *Polym. Chem.* **2010**, *1*, 1171.
43. Hadjichristidis, N.; Pitsikalis, M.; Pispas, S.; Iatrou, H. Polymers with Complex Architecture by Living Anionic Polymerization. *Chem. Rev.* **2001**, *101*, 3747–3792.
44. Hawker, C. J.; Wooley, K. L. The Convergence of Synthetic Organic and Polymer Chemistries. *Science* **2005**, *309*, 1200–1205.
45. Braunecker, W. A.; Matyjaszewski, K. Controlled/Living Radical Polymerization: Features, Developments, and Perspectives. *Prog. Polym. Sci.* **2007**, *32*, 93–146.
46. Zhu, L.; Cheng, S. Z. D.; Calhoun, B. H.; Ge, Q.; Quirk, R. P.; Thomas, E. L.; Hsiao, B. S.; Yeh, F.; Lotz, B. Phase Structures and Morphologies Determined by Self-Organization, Vitrification, and Crystallization: Confined Crystallization in an Ordered Lamellar Phase of PEO-*b*-PS Diblock Copolymer. *Polymer* **2001**, *42*, 5829–5839.
47. Hamilton, B. D.; Ha, J. M.; Hillmyer, M. A.; Ward, M. D. Manipulating Crystal Growth and Polymorphism by Confinement in Nanoscale Crystallization Chambers. *Acc. Chem. Res.* **2012**, *45*, 414–423.
48. Muller, A. J.; Balsamo, V.; Arnal, M. L.; Jakob, T.; Schmalz, H.; Abetz, V. Homogeneous Nucleation and Fractionated Crystallization in Block Copolymers. *Macromolecules* **2002**, *35*, 3048–3058.
49. Nojima, S.; Ohguma, Y.; Kadena, K.-i.; Ishizone, T.; Iwasaki, Y.; Yamaguchi, K. Crystal Orientation of Poly (ε-caprolactone) Homopolymers Confined in Cylindrical Nanodomains. *Macromolecules* **2010**, *43*, 3916–3923.

50. Nakagawa, S.; Kadena, K.-i.; Ishizone, T.; Nojima, S.; Shimizu, T.; Yamaguchi, K.; Nakahama, S. Crystallization Behavior and Crystal Orientation of Poly(ε-caprolactone) Homopolymers Confined in Nanocylinders: Effects of Nanocylinder Dimension. *Macromolecules* **2012**, *45*, 1892–1900.
51. Lazzari, M.; Scalarone, D.; Hoppe, C. E.; Vazquez-Vazquez, C.; Lopez-Quintela, M. A. Tunable Polyacrylonitrile-Based Micellar Aggregates as a Potential Tool for the Fabrication of Carbon Nanofibers. *Chem. Mater.* **2007**, *19*, 5818–5820.
52. Mohd Yusoff, S. F.; Gilroy, J. B.; Cambridge, G.; Winnik, M. A.; Manners, I. End-to-End Coupling and Network Formation Behavior of Cylindrical Block Copolymer Micelles with a Crystalline Polyferrocenylsilane Core. *J. Am. Chem. Soc.* **2011**, *133*, 11220–12230.
53. Cambridge, G.; Gonzalez-Alvarez, M. J.; Guerin, G.; Manners, I.; Winnik, M. A. Solution Self-Assembly of Blends of Crystalline-Coil Polyferrocenylsilane-block-polyisoprene with Crystallizable Polyferrocenylsilane Homopolymer. *Macromolecules* **2015**, *48*, 707–716.
54. Rizis, G.; van de Ven, T. G.; Eisenberg, A. "Raft" Formation by Two-Dimensional Self-Assembly of Block Copolymer Rod Micelles in Aqueous Solution. *Angew. Chem., Int. Ed.* **2014**, *53*, 9000–9003.
55. Sun, J. R.; Chen, X. S.; He, C. L.; Jing, X. B. Morphology and Structure of Single Crystals of Poly(ethylene glycol)-poly-(epsilon-caprolactone) Diblock Copolymers. *Macromolecules* **2006**, *39*, 3717–3719.
56. Van Horn, R. M.; Zheng, J. X.; Sun, H.-J.; Hsiao, M.-S.; Zhang, W.-B.; Dong, X.-H.; Xu, J.; Thomas, E. L.; Lotz, B.; Cheng, S. Z. D. Solution Crystallization Behavior of Crystalline−Crystalline Diblock Copolymers of Poly(ethylene oxide)-*block*-poly(ε-caprolactone). *Macromolecules* **2010**, *43*, 6113–6119.
57. Rizis, G.; van de Ven, T. G. M.; Eisenberg, A. Crystallinity-Driven Morphological Ripening Processes for Poly-(ethylene oxide)-*block*-Polycaprolactone Micelles in Water. *Soft Matter* **2014**, *10*, 2825–2835.
58. Ungar, G.; Putra, E. G. R.; de Silva, D. S. M.; Shcherbina, M. A.; Waddon, A. J. The Effect of Self-Poisoning on Crystal Morphology and Growth Rates. *Adv. Polym. Sci.* **2005**, *180*, 45–87.
59. Mohd Yusoff, S. F.; Hsiao, M.-S.; Schacher, F. H.; Winnik, M. A.; Manners, I. Formation of Lenticular Platelet Micelles *via* the Interplay of Crystallization and Chain Stretching: Solution Self-Assembly of Poly(ferrocenyldimethylsilane)-block-poly(2-vinylpyridine) with a Crystallizable Core-Forming Metalloblock. *Macromolecules* **2012**, *45*, 3883–3891.
60. Wittemann, A.; Azzam, T.; Eisenberg, A. Biocompatible Polymer Vesicles from Biamphiphilic Triblock Copolymers and their Interaction with Bovine Serum Albumin. *Langmuir* **2007**, *23*, 2224–2230.
61. Adams, D. J.; Kitchen, C.; Adams, S.; Furzeland, S.; Atkins, D.; Schuetz, P.; Fernyhough, C. M.; Tzokova, N.; Ryan, A. J.; Butler, M. F. On the Mechanism of Formation of Vesicles from Poly(ethylene oxide)-*block*-Poly(caprolactone) Copolymers. *Soft Matter* **2009**, *5*, 3086–3096.
62. Qi, W.; Ghoroghchian, P. P.; Li, G.; Hammer, D. A.; Therien, M. J. Aqueous Self-Assembly of Poly(ethylene oxide)-*block*-Poly(epsilon-caprolactone) (PEO-b-PCL) Copolymers: Disparate Diblock Copolymer Compositions Give Rise to Nano- and Meso-Scale Bilayered Vesicles. *Nanoscale* **2013**, *5*, 10908–10915.
63. Luo, L. B.; Eisenberg, A. Thermodynamic Stabilization Mechanism of Block Copolymer Vesicles. *J. Am. Chem. Soc.* **2001**, *123*, 1012–1013.
64. Yang, P. C.; Ratcliffe, L. P. D.; Armes, S. P. Efficient Synthesis of Poly(methacrylic acid)-block-Poly(styrene-alt-N-phenylmaleimide) Diblock Copolymer Lamellae Using RAFT Dispersion Polymerization. *Macromolecules* **2013**, *46*, 8545–8556.
65. Zhang, L. F.; Eisenberg, A. Crew-Cut Aggregates from Self-Assembly of Blends of Polystyrene-b-Poly(acrylic acid) Block Copolymers and Homopolystyrene in Solution. *J. Polym. Sci., Polym. Phys.* **1999**, *37*, 1469–1484.
66. Berrill, S. A.; Heatley, F.; Collett, J. H.; Attwood, D.; Booth, C.; Fairclough, J. P. A.; Ryan, A. J.; Viras, K.; Dutton, A. J.; Blundell, R. S. Chain folding in Poly(epsilon-caprolactone) studied by Small-Angle X-ray Scattering and Raman Spectroscopy. A Strategy for Blending in the Crystalline State. *J. Mater. Chem.* **1999**, *9*, 1059–1063.
67. Bogdanov, B.; Vidts, A.; Van Den Bulcke, A.; Verbeeck, R.; Schacht, E. Synthesis and Thermal Properties of Poly-(ethylene glycol)-Poly(epsilon-caprolactone) Copolymers. *Polymer* **1998**, *39*, 1631–1636.